

# Adenomyosis: three-dimensional sonographic findings of the junctional zone and correlation with histology

C. EXACOUSTOS, L. BRIENZA, A. DI GIOVANNI, B. SZABOLCS, M. E. ROMANINI, E. ZUPI and D. ARDUINI

Department of Obstetrics and Gynecology, Università degli Studi di Roma, 'Tor Vergata', Rome, Italy

**KEYWORDS:** 3D coronal plane; adenomyosis; junctional zone

## ABSTRACT

**Objective** To correlate with histopathological features the adenomyosis-induced morphological alterations of the outer myometrium and the inner myometrium ('junctional zone', JZ) detectable on two- (2D) and three-dimensional (3D) transvaginal ultrasound imaging (TVS), and to evaluate their diagnostic accuracy for adenomyosis.

**Methods** Premenopausal patients scheduled for hysterectomy for benign pathology were enrolled in this prospective study. Before hysterectomy all patients underwent detailed 2D-TV and 3D volume acquisition of the entire uterus. The major sonographic signs of adenomyosis were noted. On the multiplanar coronal and longitudinal views obtained by 3D-TV we measured the maximum and minimum JZ thickness from the basal endometrium to the internal layer of the outer myometrium (JZ<sub>max</sub>, JZ<sub>min</sub>), the difference between them (JZ<sub>dif</sub> = JZ<sub>max</sub> – JZ<sub>min</sub>) and the ratio JZ<sub>max</sub>/total maximum myometrial thickness. Results of these examinations were correlated blindly to the presence of adenomyosis on histological specimens.

**Results** A total of 72 premenopausal patients underwent 2D- and 3D-TV before hysterectomy. The histological prevalence of adenomyosis was 44.4% (32/72 patients). In diagnosing adenomyosis, the presence of myometrial cysts was the most specific 2D-TV feature (specificity, 98%; accuracy, 78%) and heterogeneous myometrium was the most sensitive (sensitivity, 88%; accuracy, 75%). The 3D-TV markers JZ<sub>dif</sub> ≥ 4 mm and JZ infiltration and distortion had high sensitivity (88%) and the best accuracy (85% and 82%, respectively). For 2D-TV and 3D-TV, respectively, the overall accuracy for diagnosis of adenomyosis was 83% and 89%, the sensitivity was 75% and 91%, the specificity was 90% and 88%, the positive predictive value was 86% and 85% and the negative predictive value was 82% and 92%.

**Conclusions** The coronal section of the uterus obtained by 3D-TV permits accurate evaluation and measurement of the JZ, and its alteration has good diagnostic accuracy for adenomyosis. Copyright © 2011 ISUOG. Published by John Wiley & Sons, Ltd.

## INTRODUCTION

Adenomyosis is a common gynecological disease, characterized by the migration of endometrial glands and stroma from the basal layer of the endometrium into the myometrium, and is associated with smooth muscle hyperplasia. Its etiology is not known, but recently there have been some interesting theories attempting to explain the association of adenomyosis with subfertility and endometriosis that consider it to be a pathology that initially affects the endomyometrial junctional zone (JZ)<sup>1,2</sup>.

The JZ is a distinct, hormone-dependent uterine compartment at the endomyometrial interface that was visualized more than 20 years ago by magnetic resonance imaging (MRI)<sup>3</sup>. This zone has been cited in the literature by many names, including archimyometrium, inner myometrium and endomyometrial junction, and correlates sonographically to the subendometrial halo or the hypoechoic tissue seen beyond the endometrial basal layer<sup>4</sup>. Despite the apparent lack of histological distinction between the JZ and the outer myometrium on light microscopy, these two zones are in reality structurally and biologically different<sup>5,6</sup>. In recent years, this endomyometrial JZ has emerged as a specialized zone, which governs many critical reproductive functions<sup>1,2,7–10</sup>.

The presence of adenomyosis causes hyperplasia and hypertrophy of myocytes surrounding heterotopic endometrial tissue that can be seen on T2-weighted

Correspondence to: Dr C. Exacoustos, Department of Obstetrics and Gynecology, Università degli Studi di Roma 'Tor Vergata', Ospedale Generale S. Giovanni Calibita 'Fatebenefratelli', Isola Tiberina 1, 00186 Rome, Italy (e-mail: caterinaexacoustos@tiscali.it)

Accepted: 28 November 2010

MRI as diffuse or focal thickening of the JZ. The heterotopic endometrial tissue may be seen as small foci of increased signal intensity in the JZ. Subjective impression of JZ irregularities is commonly used for diagnosis of adenomyosis<sup>11,12</sup>, but objective criteria are preferable. Three objective parameters have been identified for its diagnosis on MRI: thickening of the JZ  $\geq 12$  mm<sup>13–15</sup>, a ratio of maximum thickness of the JZ (JZmax)/total maximum myometrial thickness  $> 40\%$ <sup>11,15</sup>, and a difference between the JZmax and the minimum thickness of the JZ (JZmax – JZmin = JZdif)  $> 5$  mm<sup>16</sup>. While the first two criteria have been criticized the third seems to be more accurate because it is less dependent on hormonal status and menstrual cycle<sup>16</sup>.

The sonographic findings of adenomyosis described in the literature generally involve alterations of the myometrium, such as: presence of myometrial hypoechoic striations or myometrial cysts or heterogeneous areas, asymmetry of the myometrial walls, diffuse vascularity and globular uterine configuration<sup>13–21</sup>. Even with high-frequency probes (5–10 MHz), sonographic evaluation of the JZ seems to be imprecise due to the difficulty in obtaining optimal views with which to differentiate between the inner and outer myometrium. Some two-dimensional (2D) sonographic studies report only the subjective impression of a poorly defined JZ as a diagnostic criterion for adenomyosis, but with low sensitivity<sup>22,23</sup>. However, it has recently been observed that on the coronal section of the uterus, obtained with three-dimensional (3D) TVS, it is possible to visualize the JZ more clearly with certain postprocessing arrangements<sup>24</sup>.

The aim of this study was to correlate with histopathological features the adenomyosis-induced morphological alterations of the outer myometrium and the JZ detectable on 2D- and 3D-TVS, and to evaluate their diagnostic accuracy for adenomyosis.

## PATIENTS AND METHODS

In this prospective study of a consecutive series of patients, we included premenopausal women who had benign pelvic pathology (diagnosed by ultrasound or office hysteroscopy) and were scheduled for hysterectomy in our unit (Gynecology Department, Ospedale Generale S. Giovanni Calibita 'Fatebenefratelli', Università degli Studi di Roma 'Tor Vergata' Italy) from September 2008 to January 2010. Institutional review board approval for this study was obtained prior to study initiation. Informed patient consent was not required. We excluded pregnant and postmenopausal women, those with reproductive tract cancer, those on GnRH analog therapy or other hormonal therapy, and those with fibroids  $> 8$  cm in maximum diameter or more than three fibroids  $> 5$  cm in maximum diameter on ultrasound examination prior to surgery.

All patients underwent 2D, 3D and power Doppler TVS of the pelvic organs in a single examination during the secretory phase of the menstrual cycle within 2 months

before surgery. Each scan was performed by one of three expert sonographers (C.E, B.S, M.E.R.), using an E8 (GE Healthcare, Zipf, Austria) ultrasound machine equipped with a multifrequency 3D volume endovaginal probe (2.8–10 MHz). Power Doppler was used to evaluate the vascularization of the myometrial tissue. All 2D and 3D ultrasound evaluations and measurements were done during the same examination period and by the same operator. Ultrasound digital and photographic images were saved and stored on a USB drive for subsequent retrieval.

The 2D-TVS examination included evaluation and measurement of the pelvic organs. The uterus, endometrium and adnexa were evaluated for any abnormalities. The uterus and endometrium were measured and the uterine volume calculated by means of the ellipsoid formula (uterine longitudinal diameter  $\times$  transverse diameter  $\times$  anteroposterior diameter  $\times 0.532$ ). Any myometrial lesions (myomas and signs of adenomyosis) were described and measured. Specifically, in accordance with previous studies<sup>12,15–19</sup>, we determined the presence of certain TVS features associated with adenomyosis: myometrial cysts and heterogeneous areas, myometrial hypoechoic linear striations, diffuse vascularity and asymmetry of the myometrial wall. Asymmetrical myometrial walls were defined as a regular enlarged uterus with asymmetry unrelated to leiomyoma, heterogeneous myometrium as an indistinctly defined myometrial area with decreased or increased echogenicity, myometrial hypoechoic linear striations as a pattern of thin acoustic shadowing not arising from echogenic foci and/or leiomyoma, and myometrial cyst as a round anechoic area within the myometrium (Figure 1)<sup>15–21</sup>. In cases of pelvic endometriosis we assessed by TVS the extent of disease (ovaries, salpinx, rectum, sigma, bladder, uterosacral ligaments, rectovaginal septum, vagina).

Power Doppler was performed using fixed preinstalled settings: frequency, 6–9 MHz ('normal'); pulse repetition frequency, 0.6–0.3 kHz; gain, –4.0; wall motion filter, 'low 1' (40 Hz). If necessary, power Doppler gain was reduced until all color artifacts had disappeared. This modality was used to distinguish between a myometrial cyst and a vascular component, and between leiomyoma and focal adenomyosis. Localized adenomyosis and adenomyoma were characterized by the presence of rare, diffuse vessels, while fibroids had flow aligned along the external myoma capsule, appearing on imaging as a vascular ring.

Using 3D-TVS, a volume of the uterus was then acquired in order to obtain the coronal view. Two to four static gray-scale volumes of the uterus were obtained from the sagittal plane and from the transverse plane. The volume acquisition technique was standardized according to the following criteria: frequency, 6–9 MHz; magnification of the uterus up to half of the screen; sweep angle, 120°; sweep velocity, adjusted from medium to maximum quality; 3D volume box exceeding the uterus by 1 cm on each side.

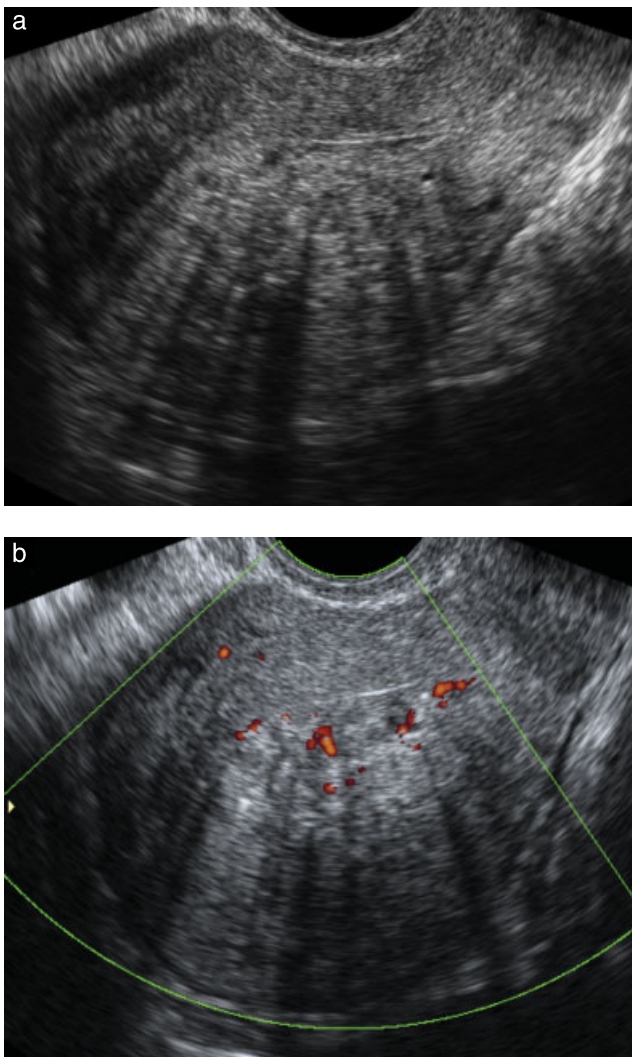


**Figure 1** Two-dimensional ultrasound imaging of a uterus in a longitudinal section showing typical sonographic features of adenomyosis. (a) Note the asymmetry of the myometrial wall (posterior thicker than anterior), and the heterogeneous myometrium with hyperechoic areas, hypoechoic striations and small cysts. (b) Few diffuse vessels can be seen on power Doppler.

The coronal view reconstruction technique involved placing a straight or curved line (OmniView or rendering mode) along the endometrial stripe on the sagittal and transverse views (Panel A and B of the multiplanar view). The multiplanar view was then manipulated until a satisfactory coronal image was obtained of the uterine external profile and the cavity, with visualization bilaterally of the interstitial portion of the Fallopian tube. Volume contrast imaging (VCI) was applied (2–4 mm slice thickness) with volume rendering (mixed light surface and gradient light). Following acquisition, ultrasound volumes were stored on the hard drive of the machine and retrieved subsequently for offline analysis.

On the coronal view the JZ appeared as a hypoechoic zone around the endometrium. Using VCI modality with 2–4-mm slices it could be viewed clearly in all planes of the multiplanar view (Figure 2), while it was poorly visualized in most (82%, 59/72) of our patients by 2D-TVS. JZ

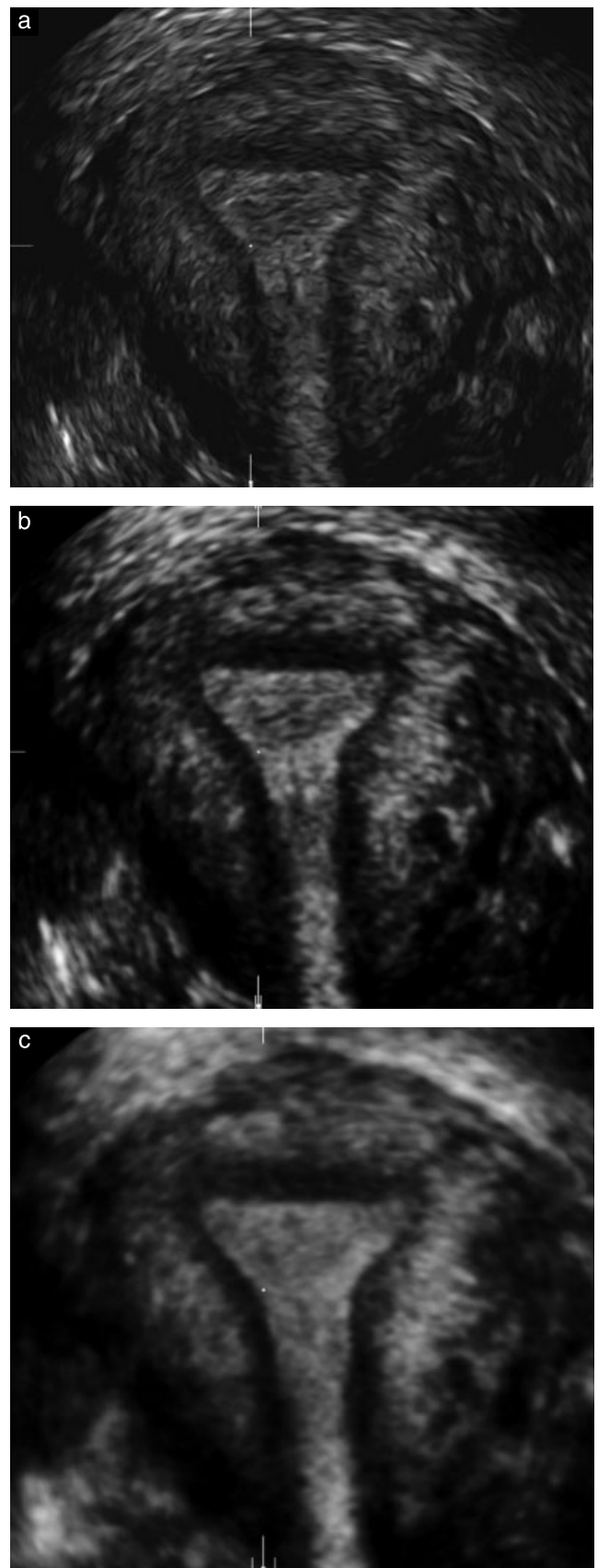


**Figure 2** Three-dimensional ultrasound imaging of a normal uterus in the coronal plane showing the endometrium, the inner myometrium (or junctional zone (JZ)) and the outer myometrium: (a) without volume contrast imaging (VCI) modality, (b) with VCI modality and slice thickness of 2 mm and (c) with VCI modality and slice thickness of 4 mm. Note the clearer view of the hypoechoic JZ with VCI modality.



**Figure 3** Three-dimensional ultrasound imaging of a normal uterus in the coronal plane showing measurement of junctional zone maximum (Calipers 1 and 4) and minimum (Caliper 3) thickness and total maximum myometrial thickness (Caliper 2).

measurements were therefore performed only on 3D multiplanar view using VCI. Disruption and infiltration of the hypoechoic JZ by the hyperechoic endometrial tissue was described and the JZ thickness was measured as the distance from the basal endometrium to the internal layer of the outer myometrium (Figure 3). We determined: JZmin (which can be considered the normal JZ thickness during any phase of the cycle not affected by adenomyosis), JZmax, the maximum myometrial thickness, presence of JZ alteration, presence of myometrial cysts, asymmetry of the myometrial wall and presence of myometrial heterogeneous areas. JZmax and JZmin were defined as the largest and smallest JZ thickness measured on coronal section or longitudinal section at any level of the uterus (fundus or anterior, posterior or lateral walls), maximum myometrial thickness as the diameter from the basal endometrium to the uterine serosa measured at the same level as that of JZmax, and alteration of the JZ as distortion and infiltration of the hypoechoic inner myometrium by hyperechoic endometrial tissue or ill-defined JZ (Figures 4 and 5); heterogeneous myometrium, myometrial hypoechoic linear striations, asymmetry and cysts were defined as for the 2D application (Figure 6). Furthermore, the JZ ratio was calculated as  $JZ_{max}/\text{total maximum myometrial thickness}$ , expressed as a percentage, and  $JZ_{dif}$  as  $JZ_{max} - JZ_{min}$ .

In all patients, hysterectomy was performed in a manner appropriate for their clinical condition (laparotomic, laparoscopic or vaginal hysterectomy). The entire uterus was sent to the pathologist, except in cases in which morcellation of the uterus had occurred.

Histopathological examination was performed by a single pathologist, who was blinded to the sonographic data and who had been specifically asked to evaluate the JZ (inner myometrium) and the outer myometrium. Histological sections encompassing the full uterine wall thickness,

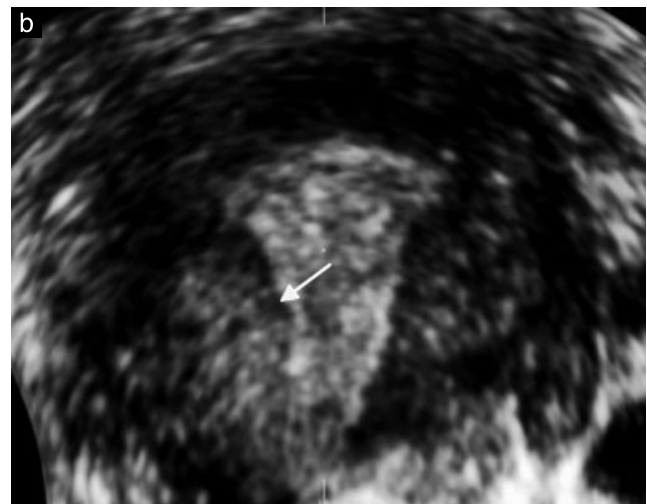


**Figure 4** Three-dimensional ultrasound imaging of uteri with adenomyosis in the coronal plane showing protrusions of the endometrium into the junctional zone (JZ). (a) Note the thicker JZ at the lateral wall and the small infiltration at the fundus (arrow) suggestive of early adenomyosis. (b) Note the complete disruption and infiltration of the JZ laterally (arrow).

from endometrium to serosa, were used for the study. In each case, at least eight slices were obtained, with at least one being from each of the fundus and the anterior, posterior and lateral walls of the uterus. Samples were also obtained from macroscopically abnormal areas of the myometrium. Adenomyosis was defined histopathologically by the presence of endometrial glands and stroma in the myometrium, located  $> 2.5$  mm beyond the endometrial junction<sup>25</sup>. In some cases it remained diffuse pathology and was evaluated by grade according to depth and number of endometrial islets in the myometrium<sup>15,25</sup>. In others it was seen as a circumscribed nodular lesion mimicking an intramural myoma, which was defined as adenomyoma. For the purposes of statistical analysis in this study, we considered only the presence or absence of adenomyosis.

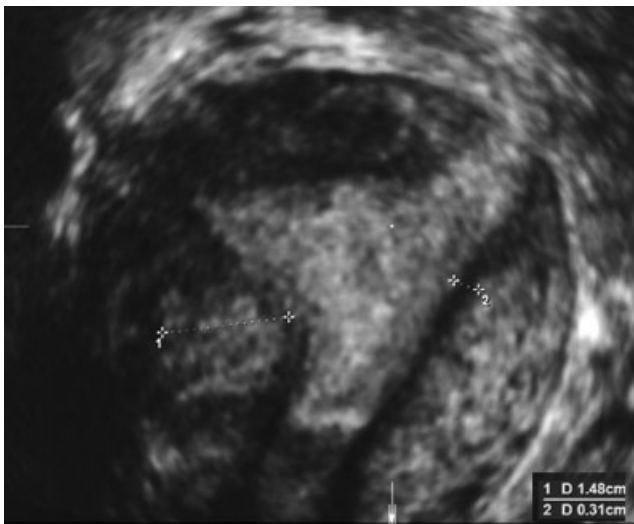


**Figure 5** Three-dimensional ultrasound imaging in the coronal plane of a uterus with adenomyosis showing measurement of junctional zone (JZ) maximum (Caliper 1) and minimum (Caliper 2) thickness. Note the complete infiltration of the JZ laterally and the distortion of the uterine cavity.

### Statistical analysis

The 2D or 3D diagnosis of adenomyosis was made based on the presence of at least two or more of any of the ultrasonographic criteria investigated. TVS findings were compared between patients with and those without uterine adenomyosis. Descriptive analysis was achieved using proportions, means and SDs. Statistical analysis

was performed using Student's *t*-test for mean and SD and proportions were compared with the chi-square test or Fisher's exact test, as appropriate.  $P < 0.05$  was considered statistically significant. Baye's theorem was used to evaluate diagnostic accuracy for adenomyosis of 2D- and 3D-TVS features. Sensitivity, specificity, accuracy, negative (NPV) and positive (PPV) predictive values and likelihood ratios (LR) were calculated.

### RESULTS

A total of 74 patients met the inclusion criteria and were enrolled into this study. Hysterectomy was performed by laparotomy in 46 patients, by laparoscopy in 19 and by vaginal hysterectomy in nine. Two patients were excluded due to morcellation of the uterus. These two patients were scheduled for total laparoscopic hysterectomy but this was converted intraoperatively to a laparoscopic supracervical hysterectomy due to adhesions. The mean age of the 72 patients included in the analysis was 46.7 (range, 38–52) years. Indications for surgery included menorrhagia or abnormal uterine bleeding in 55 (76%) patients, uterine prolapse in seven (10%) and ovarian pathology in 10 (14%). Histology of the uterus revealed diffuse adenomyosis in 32 patients, of whom 17 also had fibroids and three had associated adenomyomas. Of the 40 patients without adenomyosis, 37 had fibroids and the other three showed no myometrial pathology.

There was no statistically significant difference in the mean gravidity or parity between the group

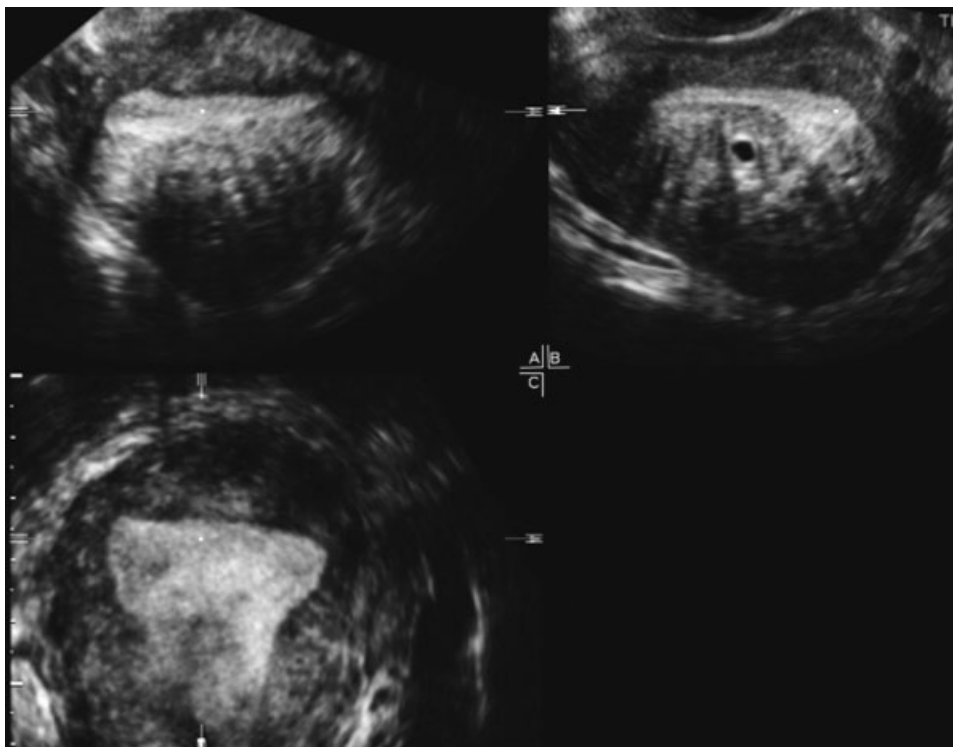


**Figure 6** Three-dimensional ultrasound imaging of a uterus with adenomyosis in multiplanar view and volume contrast imaging modality. Note it is possible in one view to see the infiltration of the junctional zone on the coronal section, and the presence of myometrial asymmetry, cysts and hyperechoic areas and hyperechoic striations in the transverse and longitudinal sections.

with adenomyosis and the group without, although patients with adenomyosis showed a tendency towards lower parity (Table 1). Dysmenorrhea occurred mostly in patients with adenomyosis, whereas menorrhagia was not statistically different between the two groups (Table 1).

The myometrial features typical of adenomyosis observed by 2D-TVS in both patients with and those without adenomyosis are reported in Table 2. Myometrial cysts, hypoechoic striations and heterogeneous myometrium were present significantly more often in uteri with adenomyosis.

The features analyzed on 3D-TVS are reported in Table 3. The mean JZmax was significantly greater in patients with adenomyosis than in those without adenomyosis, whereas the JZmin mean value was similar between the groups. The percentage of infiltration and disruption of the JZ seen on multiplanar view with VCI modality was also significantly higher in patients with compared with those without adenomyosis.

We assessed the diagnostic performance for each of the TVS findings by calculating sensitivity, specificity,

**Table 1** Population characteristics of 72 premenopausal patients prior to hysterectomy for benign pathology, according to histological diagnosis of adenomyosis

Characteristic	Adenomyosis on histology	
	Yes (n = 32)	No (n = 40)
Age (years)	46.3 ± 4.9	47.0 ± 3.6
Body mass index	24.3 ± 3.3	24.5 ± 2.9
Gravidity	1.3 ± 1.5	1.5 ± 1.3
Parity	0.8 ± 1.0	1.2 ± 0.9
Menorrhagia	81.3 (26)	72.5 (29)
Dysmenorrhea*	84.4 (27)	47.5 (19)

Data are presented as mean ± SD or % (n). \*Significant difference between those with and those without adenomyosis ( $P < 0.05$ ).

**Table 2** Two-dimensional (2D) transvaginal ultrasound (TVS) features in premenopausal patients prior to hysterectomy for benign pathology, according to histological diagnosis of adenomyosis

2D-TVS finding	Adenomyosis on histology	
	Yes (n = 32)	No (n = 40)
Uterine volume (cm <sup>3</sup> )*	206 ± 157 (152–261)	341 ± 178 (285–396)
Endometrial thickness (mm)	9.7 ± 2.2 (8.9–10.4)	9.0 ± 1.5 (8.5–9.5)
Presence of:		
Myometrial cysts*	53.1 (17)	2.5 (1)
Asymmetrical myometrium*	46.9 (15)	20.0 (8)
Hypoechoic striation*	50.0 (16)	10.0 (4)
Heterogeneous myometrium*	87.5 (28)	35.0 (14)
Endometriomas*	15.6 (5)	0
Fibroids*	53.1 (17)	92.5 (37)

Data are presented as mean ± SD (95% CI) or % (n). \*Significant difference between those with and those without adenomyosis ( $P < 0.05$ ).

PPV, NPV, positive and negative LR and accuracy (Table 4). Using presence of myometrial cysts alone as a diagnostic criterion for adenomyosis, 2D-TVS was diagnostic in 17 (53%) patients, with a high specificity of 98%, good positive LR (21.3) and negative LR (0.48) and the best accuracy (78%) of the criteria investigated. Myometrial heterogeneity alone was the most sensitive criterion (88%) and the one with the highest NPV (87%) for adenomyosis.

In evaluating the accuracy of 3D features, we first determined by receiver–operating characteristics (ROC) curve analysis the best cut-offs for JZmax (within the range 5–12 mm), JZmax/maximum myometrial thickness ratio (within the range 30–70%) and JZdif (within the range 3–8 mm). Table 4 reports the diagnostic performance for the best cut-offs; only JZmax ≥ 8 mm, JZdif ≥ 4 mm and JZ alteration showed high diagnostic accuracy.

Overall 2D- and 3D-TVS diagnosis, made based on the presence of any two or more of the individual ultrasonographic features, had an accuracy of 83% and 89%, respectively. Compared with 2D parameters, 3D parameters had statistically significantly greater sensitivity and NPV in the diagnosis of adenomyosis, but there was no significant difference in specificity, accuracy and LR.

## DISCUSSION

Pain and bleeding are symptoms typical of adenomyosis, but many women remain asymptomatic. The diagnosis is usually based on histological findings in surgical specimens. It is now widely accepted that the only two practical ways to reach a valid presurgical diagnosis are by MRI and TVS.

Several studies have illustrated that the sensitivity and specificity of 2D-TVS in diagnosing adenomyosis are comparable to those of MRI and/or histology<sup>12,14–16,18,20,26,27</sup>. While MRI analyzes features based on JZ measurements and evaluation, 2D ultrasound generally describes alterations of the outer myometrium, such as heterogeneity, hypertrophy or presence of cysts. Recently, Kepkep *et al.*<sup>28</sup> included poor definition of the JZ in their assessment of the accuracy of various 2D-TVS findings in the diagnosis of adenomyosis, and found that poor definition of the JZ had a high specificity (82%) but low sensitivity (46%) for diagnosis. One difficulty with 2D-TVS is that the JZ can be assessed in only one plane at a time and often it is not well visualized. Ahmed *et al.*<sup>29</sup> conducted a similar study to that of Kepkep *et al.*<sup>28</sup>, but also using 3D ultrasound, in which they assessed the diagnostic accuracy of ‘the presence of a hazy or ill-defined and irregular JZ on 3D coronal plane of the uterus’. They reported a PPV of 95% and an accuracy of 80% for this finding in diagnosing adenomyosis.

3D reconstruction of uterine anatomy in the coronal plane provides new and unrivaled views of the JZ<sup>24</sup>. Furthermore, using postprocessing modalities such as VCI, there is much clearer visualization of the hypoechoic

**Table 3** Three-dimensional (3D) transvaginal ultrasound (TVS) features in premenopausal patients prior to hysterectomy for benign pathology, according to histological diagnosis of adenomyosis

3D-TV <sub>S</sub> finding	Adenomyosis on histology	
	Yes (n = 32)	No (n = 40)
JZmax (mm)*	15.4 ± 8.6 (12.4–18.4)	8.0 ± 4.1 (6.7–9.3)
JZmin (mm)	6.0 ± 4.5 (4.4–7.5)	5.6 ± 3.0 (4.9–6.5)
JZdif (mm)*	9.4 ± 5.2 (7.7–11.2)	2.8 ± 2.7 (1.9–3.6)
JZmax/myom. thickness (%)*	59.3 ± 17.6 (53.2–65.4)	41.5 ± 18.2 (35.8–47.1)
Presence of:		
JZ alteration*	87.5 (28)	22.5 (9)
Myometrial cysts*	62.5 (20)	5.0 (2)
Asymmetrical myom.*	59.4 (19)	27.5 (11)
Heterogeneous myom.*	90.6 (29)	47.5 (19)

Data are presented as mean ± SD (95% CI) or % (n). \*Significant difference between those with and those without adenomyosis ( $P < 0.05$ ). JZ, junctional zone; JZdif, difference of (JZmax – JZmin); JZmax, maximum thickness of the junctional zone; JZmin, minimum thickness of the junctional zone; myom., myometrium.

JZ in comparison to that on 2D imaging (Figure 2). By obtaining coronal views of the uterine cavity, it is possible to assess the lateral and fundal aspects of the JZ, which are impossible to visualize clearly on standard 2D imaging. The ability to see the entire lateral borders of the JZ in a single view greatly increased our ability to identify minor changes and therefore to evaluate by TVS not only the outer but also the inner myometrium. To avoid the subjective evaluation of 'irregular JZ', we used on 3D-TV<sub>S</sub> of the JZ the same objective parameters that radiologists generally consider for the diagnosis of adenomyosis by MRI<sup>12,14,15</sup>. The advantage of measuring the JZ thickness is having objective parameters for comparison. Comparing 3D-TV<sub>S</sub> features to histology of the uterus after hysterectomy, we determined that JZmax ≥ 8 mm and JZdif ≥ 4 mm were significantly more accurate in diagnosing adenomyosis than were 2D features. Also, we found the subjective evaluation of infiltration and disruption by endometrial tissue in the JZ to be a very accurate tool for the diagnosis of adenomyosis.

Thickening and disruption of the JZ is strongly associated with uterine adenomyosis. Notably, adenomyosis is not a uniform disease but represents a spectrum of lesions, ranging from disruption of the JZ architecture, with little

**Table 4** Accuracy in diagnosing adenomyosis of individual two- (2D) and three-dimensional (3D) transvaginal sonographic (TVS) features and accuracy of 2D- and 3D-TV<sub>S</sub> overall

TV <sub>S</sub> finding	Sens. (% (95% CI))	Spec. (% (95% CI))	PPV (% (95% CI))	NPV (% (95% CI))	LR+ (95% CI)	LR– (95% CI)	Accuracy (% (95% CI))
<b>2D-TV<sub>S</sub></b>							
Myometrial cysts	53 (35–70)	98 (85–100)	94 (70–100)	72 (58–83)	21.3 (3.0–151.2)	0.48 (0.33–0.69)	78 (67–86)
Asymmetrical myom.	47 (30–65)	80 (64–90)	65 (43–83)	65 (50–78)	2.3 (1.1–4.8)	0.66 (0.47–0.93)	65 (54–75)
Hypoechoic striations	50 (32–68)	90 (75–97)	80 (56–93)	69 (55–81)	5.0 (1.9–13.5)	0.56 (0.39–0.79)	72 (61–81)
Heterogeneous myom.	88 (70–95)	65 (48–79)	67 (50–80)	87 (68–96)	2.5 (1.6–3.9)	0.19 (0.08–0.49)	75 (64–84)
<b>3D-TV<sub>S</sub></b>							
JZmax ≥ 8 mm	84 (67–94)	75 (58–87)	73 (56–86)	86 (69–95)	3.4 (1.9–5.9)	0.21 (0.09–0.47)	79 (68–87)
JZmax – JZmin ≥ 4 mm	88 (70–96)	83 (67–92)	80 (63–91)	89 (74–97)	5.0 (2.5–9.9)	0.15 (0.06–0.38)	85 (75–91)
JZ ratio ≥ 50%	78 (60–90)	65 (48–79)	64 (47–78)	79 (61–90)	2.2 (1.4–3.5)	0.34 (0.17–0.66)	71 (60–80)
JZ alteration	88 (70–96)	78 (61–89)	76 (58–88)	89 (72–96)	3.9 (2.2–7.0)	0.16 (0.06–0.41)	82 (72–89)
Myometrial cysts	63 (44–78)	95 (82–99)	91 (69–98)	76 (62–87)	12.5 (3.1–49.6)	0.40 (0.25–0.62)	81 (70–88)
Asymmetrical myom.	59 (4–76)	73 (56–85)	63 (44–80)	69 (53–82)	2.2 (1.2–3.9)	0.56 (0.36–0.87)	67 (55–76)
Heterogeneous myom.	91 (74–98)	53 (36–68)	60 (45–74)	88 (67–97)	1.9 (1.4–2.7)	0.18 (0.06–0.55)	69 (58–79)
<b>Overall*</b>							
2D-TV <sub>S</sub>	75 (56–88)	90 (75–97)	86 (66–95)	82 (66–91)	7.5 (2.9–19.4)	0.28 (0.15–0.51)	83 (73–90)
3D-TV <sub>S</sub>	91 (74–97)	88 (72–95)	85 (68–94)	92 (78–98)	7.3 (3.2–16.6)	0.11 (0.03–0.31)	89 (80–94)

\*Overall 2D- and 3D-TV<sub>S</sub> diagnosis was based on the presence of any two or more of the individual ultrasonographic features. JZ, junctional zone; JZmax, maximum thickness of the junctional zone; JZmin, minimum thickness of the junctional zone; JZ ratio, JZmax/total maximum myometrial thickness, expressed as %; LR+, positive likelihood ratio; LR–, negative likelihood ratio; myom., myometrium; NPV, negative predictive value; PPV, positive predictive value; Sens., sensitivity; Spec., specificity.

or no endometrial invasion, to overt diffuse adenomyosis and focal adenomyomas<sup>30,31</sup>. Modification of JZ thickness and protrusion of the endometrium into the inner myometrium could represent an early stage in the development of adenomyosis. Conventional 2D-TVS findings such as myometrial cysts and asymmetrical myometrium are more likely to represent signs of advanced disease. Considering the hypothesis that adenomyosis is most likely caused by 'invasion' of endometrial tissue across the JZ and into the myometrium, it is probably that 3D-TVS evaluation of the JZ could detect initial adenomyosis. It has been observed that in the non-pregnant uterus, highly specialized contraction waves originate exclusively from the JZ and participate in the regulation of diverse reproductive events, such as sperm transport, embryo implantation and hemostasis during menstruation<sup>32–34</sup>. Conversely, there is growing evidence to suggest that disruption of the normal JZ architecture associated with hyperplasia (which seems to precede adenomyosis) and adenomyosis inevitably alter the coordinated peristaltic activity of the inner myometrium<sup>35</sup>. This dysfunctional peristalsis and hyperperistalsis could affect sperm transport and implantation, contributing to fertility problems. They have also been linked to other pathological symptoms, such as dysmenorrhea and menorrhagia, and seem to play an integral part in the pathogenesis of endometriosis by facilitating retrograde menstruation and implantation of viable endometrial cells into the abdominal cavity<sup>36</sup>. Pelvic endometriosis, especially in its severe stages, is also strongly associated with JZ thickening<sup>37–39</sup>. On the basis of prepregnancy imaging, a recent study reported that adenomyosis is an important risk factor for spontaneous preterm delivery and preterm premature rupture of the membranes<sup>40</sup>. All these observational studies suggest that perturbations in JZ structure or function prior to conception predispose towards a spectrum of fertility and obstetric complications<sup>9,41</sup>.

Therefore, evaluation of the JZ and its alterations by non-invasive imaging could be very important, especially in patients with fertility problems. TVS is the imaging technique most commonly available in gynecological offices and therefore it, rather than MRI, is the first-line diagnostic tool for the diagnosis of adenomyosis. Our results suggest that 3D-TVS is more accurate than is conventional 2D imaging to detect adenomyosis and we propose its use to evaluate early stages of the disease, especially in young patients in whom histological diagnosis is difficult to perform.

One limitation of our study is the fact that histology was obtained from a study population of patients requiring hysterectomy, who by definition tend to be older and symptomatic, and in whom adenomyosis is likely to be more advanced. A second potential limitation of this study is the exclusion of patients with large or multiple fibroids, in whom adenomyosis is difficult to detect, even by MRI<sup>42</sup>. However, in most of these patients, the presence or absence of adenomyosis does not significantly modify surgical or medical management. Another limitation of this study was that histological biopsies were not

performed using an ultrasound-guided approach, so it was not possible to ascertain whether the JZ alterations seen on TVS were really due to adenomyosis.

In conclusion, we have shown that patients who underwent hysterectomy and had subsequent histological findings of uterine adenomyosis had, on the 3D coronal view, a thicker and altered JZ compared with patients without adenomyosis. Further study is needed to determine JZ TVS features in younger fertile and infertile patients and to correlate these findings to histological ultrasound-guided biopsies.

## REFERENCES

- Kissler S, Zangos S, Kohl J, Wiegatz I, Rody A, Gaetje R, Vogl TJ, Kunz G, Leyendecker G, Kaufmann M. Duration of dysmenorrhoea and extent of adenomyosis visualised by magnetic resonance imaging. *Eur J Obstet Gynecol Reprod Biol* 2008; **137**: 204–209.
- Leyendecker G, Wildt L, Mall G. The pathophysiology of endometriosis and adenomyosis: tissue injury and repair. *Arch Gynecol Obstet* 2009; **280**: 529–538.
- Benagiano G, Brosens I. History of adenomyosis. *Best Pract Res Clin Obstet Gynaecol* 2006; **20**: 449–463.
- Gordts S, Brosens JJ, Fusi L, Benagiano G, Brosens I. Uterine adenomyosis: a need for uniform terminology and consensus classification. *Reprod Biomed Online* 2008; **17**: 244–248.
- McCarthy S, Scott G, Majumdar S, Shapiro B, Thompson S, Lange R. Uterine junctional zone: MR study of water content and relaxation properties. *Radiology* 1989; **171**: 241–243.
- Mehasseb MK, Bell SC, Pringle JH, Habiba MA. Uterine adenomyosis is associated with ultrastructural features of altered contractility in the inner myometrium. *Fertil Steril* 2010; **93**: 2130–2136.
- Brosens JJ, de Souza NM, Barker FG. Uterine junctional zone: function and disease. *Lancet* 1995; **346**: 558–560.
- Brosens JJ, Barker FG, de Souza NM. Myometrial zonal differentiation and uterine junctional zone hyperplasia in the non-pregnant uterus. *Hum Reprod Update* 1998; **4**: 496–502.
- Brosens I, Derwig I, Brosens J, Fusi L, Benagiano G, Pijnenborg R. The enigmatic uterine junctional zone: the missing link between reproductive disorders and major obstetrical disorders? *Hum Reprod* 2010; **3**: 569–574.
- Fusi L. The uterine junctional zone. *Best Pract Res Clin Obstet Gynaecol* 2006; **20**: 479–491.
- Ascher SM, Arnold LL, Patt RH, Schrufer JJ, Bagley A, Semelka RCR, Zeman RK, Simon JA. Adenomyosis: prospective comparison of MR imaging and transvaginal sonography. *Radiology* 1994; **190**: 803–806.
- Reinhold C, McCarthy S, Bret PM, Mehio A, Atri M, Zakarian R, Glaude Y, Liang L, Seymour RJ. Diffuse adenomyosis: comparison of endovaginal US and MR imaging with histopathologic correlation. *Radiology* 1996; **199**: 151–158.
- Reinhold C, Tafazoli F, Wang L. Imaging features of adenomyosis. *Hum Reprod Update* 1998; **4**: 337–349.
- Dueholm M, Lundorf E. Transvaginal ultrasound or MRI for diagnosis of adenomyosis. *Curr Opin Obstet Gynecol* 2007; **19**: 505–512.
- Bazot M, Cortez A, Darai E, Rouger J, Chopier J, Antoine JM, Uzan S. Ultrasonography compared with magnetic resonance imaging for the diagnosis of adenomyosis: correlation with histopathology. *Hum Reprod* 2001; **16**: 2427–2433.
- Dueholm M, Lundorf E, Hansen ES, Ledertoug S, Sorensen JS, Olesen F. Magnetic resonance imaging and transvaginal ultrasonography for diagnosis of adenomyosis. *Fertil Steril* 2001; **76**: 588–594.
- Fedele L, Bianchi S, Dorta M, Arcaini L, Zanotti F, Carinelli S. Transvaginal ultrasonography in the diagnosis of diffuse adenomyosis. *Fertil Steril* 1992; **58**: 94–97.



18. Bromley B, Shipp TD, Benacerraf B. Adenomyosis: sonographic findings and diagnostic accuracy. *J Ultrasound Med* 2000; **19**: 529–534.
19. Reinhold C, Atri M, Mehio A, Zakarian R, Aldis AE, Bret PM. Diffuse uterine adenomyosis: morphologic criteria and diagnostic accuracy of endovaginal sonography. *Radiology* 1995; **197**: 609–614.
20. Dueholm M. Transvaginal ultrasound for diagnosis of adenomyosis: a review. *Best Pract Res Clin Obstet Gynaecol* 2006; **20**: 569–582.
21. Brosens JJ, de Souza NM, Barker FG, Paraschos T, Winston RM. Endovaginal ultrasonography in the diagnosis of adenomyosis uteri: identifying the predictive characteristics. *Br J Obstet Gynaecol* 1995; **102**: 471–474.
22. Atri M, Reinhold C, Mehio AR, Chapman WB, Bret PM. Adenomyosis: US features with histologic correlation in an in-vitro study. *Radiology* 2000; **215**: 783–790.
23. Hulka CA, Hall DA, McCarthy K, Simeone J. Sonographic findings in patients with adenomyosis: can sonography assist in predicting extent of disease? *AJR Am J Roentgenol* 2002; **179**: 379–383.
24. Naftalin J, Jurkovic D. The endometrial-myometrial junction: a fresh look at a busy crossing. *Ultrasound Obstet Gynecol* 2009; **34**: 1–11.
25. Zaloudek C, Norris HJ. Mesenchymal tumors of the uterus. In *Blaustein's Pathology of the Female Genital Tract*, 4<sup>th</sup> edn, Kurmann RJ (ed.). Springer-Verlag: New York, 1994; 487–452.
26. Bazot M, Dara E, Rouger J, Detchev R, Cortez A, Uzan S. Limitations of transvaginal sonography for the diagnosis of adenomyosis, with histopathological correlation. *Ultrasound Obstet Gynecol* 2002; **20**: 603–611.
27. Vercellini P, Cortesi I, De Giorgi O, Merlo D, Carinelli SG, Crosignani PG. Transvaginal ultrasonography versus uterine needle biopsy in the diagnosis of diffuse adenomyosis. *Hum Reprod* 1998; **13**: 2884–2887.
28. Kepke K, Tuncay YA, Goynumer G, Tatal E. Transvaginal sonography in the diagnosis of adenomyosis: which findings are most accurate? *Ultrasound Gynecol Obstet* 2007; **30**: 341–345.
29. Ahmed AI, Mahmoud AEA, Fadiel AA, Frederick N. Comparison of 2-, 3D and Doppler ultrasound with histological findings in adenomyosis. *Fertil Steril* 2007 (Suppl 1); **88**: S82.
30. Vercellini P, Viganò P, Somigliana E, Daguati R, Abbiati A, Fedele L. Adenomyosis: epidemiological factors. *Best Pract Res Clin Obstet Gynaecol* 2006; **20**: 465–477.
31. Ferenczy A. Pathophysiology of adenomyosis. *Hum Reprod Update* 1998; **4**: 312–322.
32. De Vries K, Lyons EA, Ballard G. Contractions of the inner third of the myometrium. *Am J Obstet Gynecol* 1990; **162**: 679–682.
33. Leyendecker G, Kunz G, Herbertz M, Beil D, Huppert P, Mall G, Kissler S, Noe M, Wildt L. Uterine peristaltic activity and development of endometriosis. *Ann N Y Acad Sci* 2004; **1034**: 338–355.
34. Fanchin R, Righini C, Olivennes F, Taylor S, de Ziegler D, Frydman R. Uterine contractions at the time of embryo transfer alter pregnancy rates after in-vitro fertilization. *Hum Reprod* 1998; **13**: 1968–1974.
35. Kunz G, Herbertz M, Beil D, Huppert P, Leyendecker G. Adenomyosis as a disorder of the early and late human reproductive period. *Reprod BioMed Online* 2007; **15**: 681–685.
36. Bulletti C, De Ziegler D, Polli V, Del Ferro E, Palini S, Flamigni C. Characteristics of uterine contractility during menses in women with mild to moderate endometriosis. *Fertil Steril* 2002; **77**: 1156–1161.
37. Devlieger R, D'Hooghe T, Timmerman D. Uterine adenomyosis in the infertility clinic. *Hum Reprod Update* 2003; **9**: 139–147.
38. Kunz G, Beil D, Huppert P, Noe M, Kissler S, Leyendecker G. Adenomyosis in endometriosis- prevalence and impact on fertility. Evidence from magnetic resonance imaging. *Hum Reprod* 2005; **20**: 2309–2316.
39. Landi S, Mereu L, Pontrelli G, Stepniewska A, Romano L, Tateo S, Dorizzi C, Minelli L. The influence of adenomyosis in patients laparoscopically treated for deep endometriosis. *J Minim Invasive Gynecol* 2008; **15**: 566–570.
40. Juang CM, Chou P, Yen MS, Twu NF, Horng HC, Hsu WL. Adenomyosis and risk of preterm delivery. *BJOG* 2007; **114**: 165–169.
41. Tocci A, Greco E, Ubaldi FM. Adenomyosis and 'endometrial-subendometrial myometrium unit disruption disease' are two different entities. *Reprod BioMed Online* 2008; **2**: 281–291.
42. Moghadam R, Lathi RB, Shahmohamady B, Saperi NS, Nezhat CH, Nezhat F, Nezhat C. Predictive value of magnetic resonance imaging in differentiating between leiomyoma and adenomyosis. *JSLs* 2006; **10**: 216–219.